Design Method for Butter–Cheby Bandpass Filters With Even Number of Resonators

Hee-Ran Ahn, *Senior Member, IEEE*, and Sangwook Nam, *Senior Member, IEEE*

***Abstract*—A design method for the bandpass filters with even number of resonators is presented for compacter size and wider bandwidth. The design method is based on the conventional filters with two resonators defined as a scattering parameter at a given frequency and a characteristic impedance of a 0° lumped-element equivalent circuit. The filter designed in this paper can be terminated in equal impedances and may have ripple responses at the same time for the wider bandwidths. Since the filter suggested in this paper has advantages that both Butterworth and Chebyshev filters possess, it is called a Butter–Cheby filter to distinguish from conventional filters. For better performance of the Butter–Cheby filter, a way to make transmission zeros is also discussed. To verify the design method, a Butter–Cheby filter with four resonators having 0.01-dB ripple is fabricated with distributed and lumped elements and measured at a design center frequency of 1 GHz. The measured results are in good agreement with the prediction, achieving less than 0.4-dB insertion loss, more than 20-dB return loss, and a transmission zero of 2 GHz.**

***Index Terms*—Butter–Cheby bandpass filters (BPFs), Butterworth and Chebyshev filters, design method of wideband filters, lumped-element BPFs.**

I. Introduction

FOR WIRELESS communication systems, remarkable improvements have been achieved in reducing mass and volume. A significant portion of such improvement has come from numerous innovations in the design of microwave filters and multiplexers [1]–[7]. The multiplexer, consisting of several filters, is indispensable for compact-sized front-end design and has therefore received substantial attention from circuit designers. For the various applications of the multiplexers, the bandpass filter (BPF) design is important and the name of the BPFs is determined depending on which filtering functions being used. They are Bessel [8], [9] Butterworth, Chebyshev [10], and Jacobian elliptic filters [11]. The Bessel and Butterworth filters have maximally flat response in the passband. The Chebyshev-type 1 or 2 filters have ripples in the passband or stopband, respectively. The elliptic filter has ripples in both passband and stopband. If no ripple of the elliptic filters is assumed in the stopband, the filter characteristics are very similar to those of the Chebyshev-type 1 filter. The Chebyshev filter in this paper is meant as the Chebyshev-type 1 filter hereafter.

Manuscript received October 25, 2011; revised January 19, 2012; accepted January 26, 2012. Date of publication April 04, 2012; date of current version May 25, 2012. This work was supported by the Korea Government [Ministry of Education, Science and Technology (MEST)] under National Research Foundation of Korea (NRF) Grant 2011-0001270.

The authors are with the School of Electrical Engineering and Computer Science, Seoul National University, Seoul 151-742, Korea (e-mail: hranahn@gmail.com; snam@snu.ac.kr).

Color versions of one or more of the figures in this paper are available online at http://ieeexplore.ieee.org.

Digital Object Identifier 10.1109/TMTT.2012.2189122

If the number of resonators of the BPF is even, it has advantages to build multiplexers [1], [2]. With even-order n, the Butterworth low-pass prototype is terminated in equal impedances, but no ripple response is possible. The Chebyshev filter is able to have ripple responses, but equal termination impedances are impossible. If both ripple response and equal termination impedances are needed at the same time, additional J- or K-inverters like 90° (270°) transmission-line sections, gaps, discontinuities, or coupling structures are required for the Chebyshev BPF responses [12].

In this paper, a design method for the BPFs with an even number of resonators is presented to have equal termination impedances for compacter size and ripples for wider bandwidth without any additional impedance (admittance) inverter. All the poles of the Chebyshev filter with an even number of resonators are located at different frequencies where perfect matching can be achieved, and no pole exists at the design center frequency, which is the reason why the termination impedances should be different. On the other hand, all the poles of the Butterworth filters are located at a design center frequency, which is the reason why perfect matching can be achieved at a design center frequency. In order that any filter with an even number of resonators can be terminated in equal termination impedances and may have ripple response at the same time, at least two poles should be located at a design center frequency, and the rest of poles should be placed outside of the center frequency to have ripple responses. For this, a method how to split the poles overlapped at the design center frequency to outside of the center frequency is suggested by using a relation between a characteristic impedance of 0° lumped-element equivalent circuit (0° LEC) and the element values of Butterworth low-pass prototype. The 0° LEC will be derived later. The resulting filter does not belong to either Butterworth or Chebyshev filters. Thus, the filters suggested in this paper are called Butter–Cheby filters to distinguish from the conventional filters. Several examples of the Butter–Cheby filters with $n = 2$–10 are demonstrated, and a way to make transmission zeros is treated for better filter performance. To verify the design method, a Butter–Cheby filter with $n = 4$ is fabricated on a substrate (RT/Duroid 5870, $\varepsilon_r = 2.33, H = 0.787$ mm) with lumped and distributed elements. Measured results are in good agreement with the predicted ones.

II. Filters With Even Number of Resonators

A. Suitable Number of Resonators

To design a channel filter in a multiplexer, the number of resonators may be determined in accordance with the filter

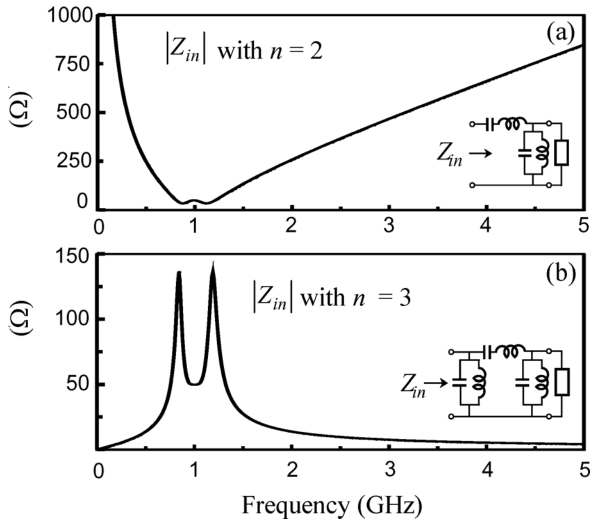

Fig. 1. Input impedances of two types of filters. (a) Two resonators. (b) Three resonators.

TABLE I
INPUT IMPEDANCES OF BUTTERWORTH BPFs WITH $n = 2$ AND 3

GHz	0.5	0.84	1	3	5
$n = 2$	256.1 Ω	42.4 Ω	50 Ω	466.2 Ω	845.6 Ω
$n = 3$	13.8 Ω	136.2 Ω	50 Ω	7.59 Ω	4.18Ω

performance required. All the channel filters designed to meet the requirement are connected to build a multiplexer, and conventional designs of the multiplexers include common port approaches [3]–[5], [7] that all the channel filters are connected at a common port in parallel [3]–[5], [7] or in series. In the case of the parallel connection, if the input impedance of the channel filter is near open-circuited at the resonance frequencies of other channel filters, it is advantageous to build the multiplexer [1], [2].

Two Butterworth filters with two and three resonators are designed at 1 GHz, and absolute values of the input impedance $|Z_{\rm in}|$ are calculated/compared in Fig. 1 and in Table I where n is the number of resonators. In this case, fractional bandwidth and termination impedances of both filters are 0.4 and 50 Ω. At a design center frequency of 1 GHz, the input impedances of both filters are equally 50 Ω. At 0.84 GHz, close to the center frequency of 1 GHz, the input impedance with $n = 3$ is 136.2 Ω, while that with $n = 2$ is 42.4 Ω. At 0.5 GHz, slightly outside of the center frequency, that with $n = 3$ is 13.8 Ω, whereas 256.1 Ω with $n = 2$. At 3 and 5 GHz, those with $n = 2$ are 466.2 and 845.6 Ω, while those with $n = 3$ are 7.58 and 4.18 Ω. The filter with two resonators are near open circuit even slightly outside of the design center frequency, which may be advantageous for the multiplexers, whereas those with $n = 3$ are near short circuit. Due to the advantage of the BPFs with an even number of resonators, the filters with n even will be investigated.

B. Butter–Cheby Filters

The low-pass prototype is, in general, defined as the low-pass filter, of which the element values are normalized to source resistance or conductance to make the source resistance or conductance equal to unity, defined by $g_0 = 1$ and g_{n+1}. With even order n, the two termination impedances (source and load) should be different for the Chebyshev filters, but equal to each other for the Butterworth filters. In this paper, new types of filters having both advantages that Chebyshev and Butterworth filters possess will be discussed. That is, the filters with even order n can be terminated in equal termination impedances and may have ripple responses. The filters are called Butter–Cheby filters to distinguish from the conventional Butterworth or Chebyshev filters.

For example, with $n = 4$, the Chebyshev filter has four poles located at different frequencies, by which ripples are generated. The ripple characteristics may be explained from the Butterworth filter whose four poles are overlapped at a design center frequency. Fig. 2 explains the pole locations and frequency responses of S_{11} where those of the Chebyshev filter are in Fig. 2(a) and (b) and those of the Butter–Cheby filter are in Fig. 2(c) and (d). To have the Chebyshev ripple response, two of four poles of the Butterworth filter overlapped at a design center frequency are separated from the center frequency to the right and left frequencies by $Chd\ 1$ and $Chd\ 2$, as detailed in Fig. 2(a), where f_0 is a design center frequency. The remaining two poles are also split in a similar way by $Chd\ 3$ and $Chd\ 4$. The frequency distances of $Chd\ 1$ and $Chd\ 2$ are approximately the same, but not equal to each other. So do those of $Chd\ 3$ and $Chd\ 4$. The resulting frequency response is plotted in Fig. 2(b) where almost perfect matching appears at the pole locations, but does not at f_0. Due to the ripple, the Chebyshev filter has steeper roll-off and wider bandwidth. The termination impedances should, however, be different with $n = 4$. To have the same termination impedances of the Chebyshev filter, additional J- or K-inverters like 90° (270°) transmission-line sections, gaps, discontinuities, and coupling structures are needed.

Just like the ripple of the Chebyshev filter was elucidated, the ripple may be produced by using the Butterworth design method to have equal termination impedances and wider bandwidth. For the equal termination impedances to be possible, two of four poles are left at the center frequency, and two others are moved to the right and left frequencies by $BCd\ 1$ and $BCd\ 2$ in Fig. 2(c). The consequential frequency response is plotted in Fig. 2(d). The way to generate ripples by moving the poles overlapped at a center frequency will be discussed using the characteristic impedance of 0° LEC of a transmission-line section and a conventional design method of the BPFs with two resonators [1].

III. FILTER DESIGNS

A. 0° Lumped-Element Equivalent Circuit

A transmission-line section with a characteristic impedance of Z_T and electrical length of $2\Theta > 0$ is depicted in Fig. 3(a), and its lumped-element equivalent circuit in Fig. 3(b) [13]. For the transmission-line section in Fig. 3(a), the even- and odd-mode impedances are

$$Z_{OC} = -jZ_T \cot\Theta \quad (1a)$$

$$Z_{SC} = jZ_T \tan\Theta. \quad (1b)$$

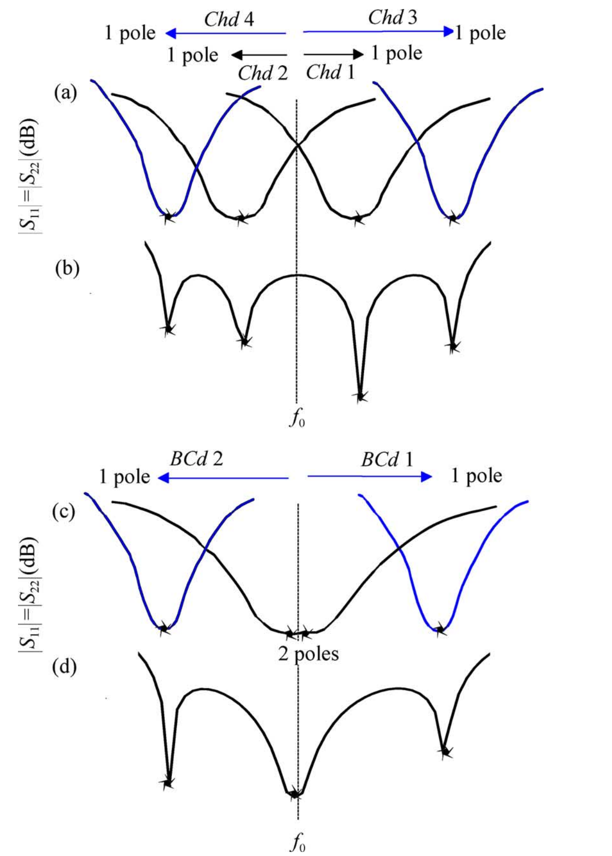

Fig. 2. Pole locations and resulting frequency responses of $|S_{11}|$. (a) Pole location of Chebychev filter. (b) Frequency response of the Chebychev filter. (c) Pole location of Butter–Cheby filter. (d) Frequency response of the Butter–Cheby filter.

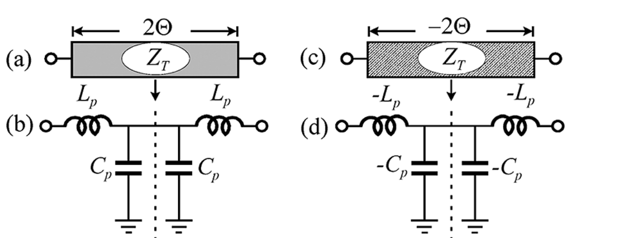

Fig. 3. Equivalent circuits of transmission-line sections with a characteristic impedance of Z_T. (a) Transmission-line section with electrical length of $2\Theta > 0$. (b) Lumped-element equivalent circuit with 2Θ. (c) Transmission-line section with electrical length of -2Θ. (d) Lumped-element equivalent circuit with -2Θ.

In the lumped-element equivalent circuit in Fig. 3(b), the even- and odd-mode impedances are

$$Z_{OC} = j\left(\omega L_p - \frac{1}{\omega C_p}\right) \tag{2a}$$

$$Z_{SC} = j\omega L_p. \tag{2b}$$

From the two sets of equations in (1) and (2), the inductance and capacitance in Fig. 3(b) are computed as

$$\omega L_p = Z_T \tan\Theta \tag{3a}$$

$$\omega C_p = \frac{\sin 2\Theta}{2Z_T}. \tag{3b}$$

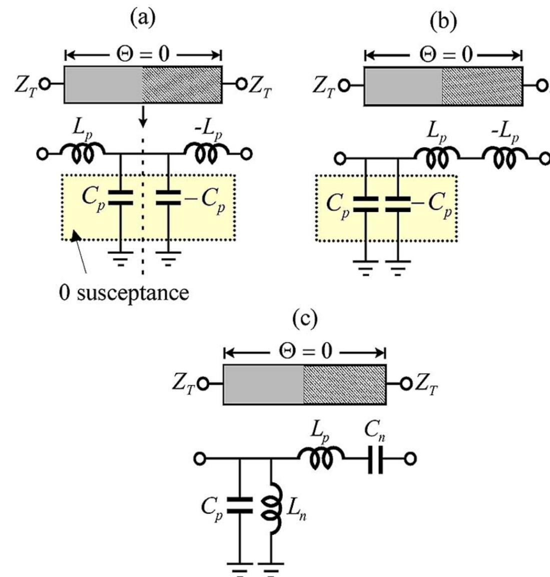

Fig. 4. 0° LEC. (a) Connecting two half circuits with positive and negative electrical lengths. (b) Moving the positive inductance of L_p close to $-L_p$. (c) Final circuit of 0° LEC.

For -2Θ in Fig. 3(c), substituting $-\Theta$ into Θ in (3) results in $-L_p$ and $-C_p$ in Fig. 3(d).

Connecting in cascade two halves of each transmission-line section with positive or negative electrical length results in zero phase delay of a transmission-line section, as described in Fig. 4(a). Since a parallel connection of C_p and $-C_p$ results in 0 susceptance, the inductance of L_p can be moved close to $-L_p$ like the circuit in Fig. 4(b). Negative reactance of $-\omega L_p$ and negative susceptance of $-\omega C_p$ become positive susceptance and positive reactance such as

$$j\omega(-L_p) = \frac{1}{j\omega C_n} \tag{4a}$$

$$j\omega(-C_p) = \frac{1}{j\omega L_n}. \tag{4b}$$

Applying the relation in (4), the final circuit of 0° LEC is obtained as that in Fig. 4(c). Associated with angular resonance frequency of ω_0, the following relation yields:

$$L_p C_n = C_p L_n = \frac{1}{\omega_0^2}. \tag{5}$$

The characteristic impedance Z_T of the transmission-line section in Fig. 4 is

$$Z_T = \sqrt{\frac{L_p}{C_p}}\sqrt{\frac{\sin 2\Theta}{2\tan\Theta}}. \tag{6}$$

With the length of Θ close to 0 in (6), the characteristic impedance Z_T of the transmission line section in Fig. 4 becomes Z_{T0} and the value is

$$Z_{T0} = \lim_{\theta\to 0} Z_T = \sqrt{\frac{L_p}{C_p}} = \sqrt{\frac{L_n}{C_n}}. \tag{7}$$

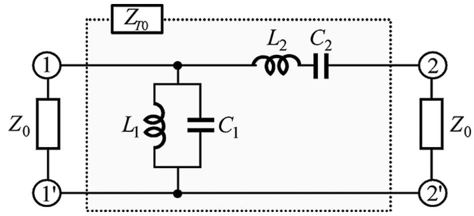

Fig. 5. BPF with $n = 2$.

B. Filter Design With $n = 2$

A BPF with $n = 2$ is described in Fig. 5 where it consists of series and shunt resonators having inductances L_1 and L_2 and capacitances C_1 and C_2. The BPF in Fig. 5 has the same form as that of 0° LEC in Fig. 4(c), and therefore is expressed with the characteristic impedance Z_{T0} of the 0° LEC. The two termination impedances are equally Z_0, and Z_{T0} is defined as $\sqrt{L_2}/\sqrt{C_1} = \sqrt{L_1}/\sqrt{C_2}$. The design equations of the BPF related with the Z_{T0} [1] are

$$L_1 = \sqrt{T(f, f_0)}Z_{T0} \quad C_1 = \frac{1}{\omega_0^2 \cdot L_1} \tag{8a}$$

$$C_2 = \frac{\sqrt{T(f, f_0)}}{Z_{T0}} \quad L_2 = \frac{1}{\omega_0^2 \cdot C_2} \tag{8b}$$

where

$$T(f, f_0) = \left\{\left(\frac{f}{f_0}\right)^2 - 1\right\}^2 \times \left\{2(2\pi f)^2 \sqrt{\frac{1}{|S_{21}(f, f_0)|^2} - 1}\right\}^{-1} \tag{9}$$

where f and f_0 are operating and resonance frequencies, and $S_{21}(f, f_0)$ is a transmission scattering parameter at a given frequency f, where $f \neq f_o$. Linking those (8) and (9) to the conventional Butterworth filter design [11], [12], [14], the characteristic impedance Z_{T0} and T in (8) and (9) are expressed as

$$T = \frac{\Delta^2}{\omega_0^2 \cdot g_1 \cdot g_2} \tag{10a}$$

$$Z_{T0} = Z_0\sqrt{\frac{g_2}{g_1}} \tag{10b}$$

where g_1 and g_2 are the element values of Butterworth low-pass prototype, $\omega_0 = 2\pi f_0$ and $\Delta = (f_2 - f_1)/f_0$ with f_1 and f_2 passband edges (3-dB insertion-loss edges).

From (9) and (10), the attenuation A of the filter is calculated as

$$A(f, f_0) = 10\log_{10}\frac{1}{|S_{21}(f, f_0)|^2} = 10\log_{10}\left[1 + \left\{\frac{g_1 \cdot g_2}{2}X(f, f_0)^2\right\}^2\right] \tag{11}$$

where $X(f, f_0)$ is $(f/f_0 - f_0/f)/\Delta$ and a mapping function to transfer a low-pass prototype into a BPF with $X(f_2, f_0) = 1$ and $X(f_1, f_0) = -1$. With $n = 2, g_1 = g_2 = 1.414$ [11], [12], [14] and the attenuation in (11) is therefore 3 dB at f_1 and f_2. In the conventional design, since the element values of

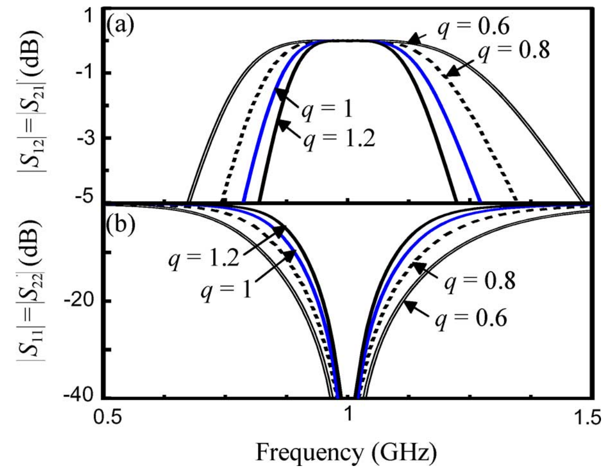

Fig. 6. Frequency responses of Butter–Cheby filters with $n = 2$. (a) $|S_{12}| = |S_{21}|$. (b) $|S_{11}| = |S_{22}|$.

g_1 and g_2 are fixed, the fractional bandwidth of Δ is only one value. The bandwidth may, however, be changeable by varying g_1 and g_2 in (11) where the fractional bandwidth Δ is inversely proportional to g_1 and g_2. As far as the termination impedances are equal to each other, perfect matching appears at a design center frequency, but the maximum bandwidth can be achieved when $Z_{T0} = Z_0$ in Fig. 5. To see the influence of g_1 and g_2 on the frequency response of the filter, the new element values g_1' and g_2' are defined as

$$g_1' = g_2' = qg_1 = qg_2 \tag{12}$$

where q is a real positive number.

Several filters were simulated at a design center frequency of 1 GHz by varying q, and the simulated frequency responses are plotted in Fig. 6. With $q = 1$, the filter is the same as the conventional Butterworth filter. With $q = 1.2$, the filter has the maximally flat response, but the 3-dB bandwidth is reduced. When $q = 0.8$, the bandwidth increases, and more bandwidths are obtained with q smaller. The bandwidth may be broadened by controlling the value of g_1' and g_2', but the return-loss performance does not seem to be better accordingly. To have both insertion- and return-loss bandwidths increased, ripples are needed for the Butterworth filter design. As explained in Fig. 2(c), two poles are required for the perfect matching at a design center frequency. Therefore, any ripple with two resonators in Fig. 5 is not easy.

C. Filter Design With $n = 4$

For n more than 2, the design equations (8)–(10) need to be generalized such as

$$L_{2i-1} = \sqrt{T_{(2i-1,2i)}}Z_{T0(2i-1,2i)} \tag{13a}$$

$$C_{2i-1} = \frac{1}{\omega_0^2 \cdot L_{2i-1}} \tag{13b}$$

$$C_{2i} = \frac{\sqrt{T_{(2i-1,2i)}}}{Z_{T0(2i-1,2i)}} \tag{13c}$$

$$L_{2i} = \frac{1}{\omega_0^2 \cdot C_{2i}} \tag{13d}$$

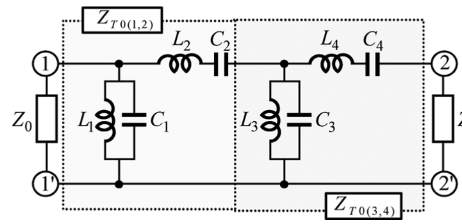

Fig. 7. BPF with $n = 4$.

where

$$T_{(2i-1,2i)} = \frac{\Delta^2}{\omega_0^2 \cdot g_{2i-1} \cdot g_{2i}} \tag{13e}$$

$$Z_{T0(2i-1,2i)} = Z_0\sqrt{\frac{g_{2i}}{g_{2i-1}}} = Z_0 R_{0(2i-1,2i)} \tag{13f}$$

where i is a positive integer and possible to $n/2$, g_{2i-1} and g_{2i} are element values of the Butterworth low-pass prototype, and $R_{0(2i-1,2i)}$ is the ratio of $Z_{T0(2i-1,2i)}$ to Z_0. With $n = 2$, the value of i is only 1. The inductances and capacitances become L_1, L_2, C_1, and C_2 in (8) and $T_{(1,2)} = T$ in (10a), $Z_{T0(1,2)} = Z_{T0}$ and $R_{0(1,2)} = \sqrt{g_2/g_1}$ in (10b).

With $n = 4$, i is 1 and 2 and two parallel and two series resonators are therefore needed as displayed in Fig. 7. The element values with $n = 4$ of the Butterworth low-pass prototype are $g_1 = g_4 = 0.7654$ and $g_2 = g_3 = 1.848$ [11], [12], [14]. The characteristic impedance $Z_{T0(1,2)}$ made by the first and second resonators (Fig. 7) is $Z_0\sqrt{g_2/g_1}$ and $Z_{T0(3,4)}$ by the third and fourth ones $Z_0\sqrt{g_4/g_3}$. In this case, $R_{0(1,2)} \cdot R_{0(3,4)} = 1$ to have perfect matching at a design center frequency. When $n = 6, g_1 = g_6 = 0.5176, g_2 = g_5 = 1.414$ and $g_3 = g_4 = 1.932$ [11], [12], [14]. The product of $R_{0(1,2)} \cdot R_{0(3,4)} \cdot R_{0(5,6)}$ is also unity. For $n = 8$, $R_{0(1,2)} \cdot R_{0(3,4)} \cdot R_{0(5,6)} \cdot R_{0(7,8)}$ is also unity. To have the ripple responses with n even, i.e., to move the poles overlapped at a design center frequency, $R_{0(2i-1,2i)}$ needs to be changed to $R_{(2i-1,2i)}$, but the following relation should be satisfied to have perfect matching at a design center frequency:

$$\prod_{i=1}^{n/2} R_{(2i-1,2i)} = 1. \tag{14}$$

With $n = 4$, to satisfy the relation in (14), $R_{(1,2)}$ and $R_{(3,4)}$ should be

$$R_{(1,2)} = p\, R_{0(1,2)} \tag{15a}$$

$$R_{(3,4)} = \frac{R_{0(3,4)}}{p} \tag{15b}$$

where p is a real positive number.

Varying p in (15), the filters with $n = 4$ and $\Delta = 0.4$ were designed at a center frequency of 1 GHz, and the calculated capacitances and inductances are written in Table II. The frequency responses are plotted in Fig. 8 where the frequency responses of $|S_{12}| = |S_{21}|$ and $|S_{11}| = |S_{22}|$ are in Fig. 8(a) and (b), respectively.

When $p = 1$, the frequency response is the same as that of the conventional Butterworth filter. When $p = 1.1$, it has the maximally flat response, but the bandwidth decreases. With $p = 0.9$ to 0.7, the filters have ripples. The frequency responses with $p < 1$ meet those with $p = 1$ at four frequencies. Two of them are located at the design center frequency, and two others are placed on the frequency response with $p = 1$, where peak values of $|S_{11}|$ between two poles [see Fig. 8(b)] exit. The two frequencies where the peak value of $|S_{11}|$ is produced are not symmetric with respect to the center frequency, because the filter itself with $p = 1$ is inherently asymmetric. When $p = 0.9$, the peak value is about -28.3 dB [see Fig. 8(b)], when $p = 0.8$, it is about -16.5 dB and when $p = 0.7$, it about -9.7 dB. With p decreasing, the peak values of $|S_{11}|$ between two poles increase. Due to the ripples in Fig. 8, the bandwidths of the filters may be enlarged, compared to those of the conventional Butterworth filter, or, $p = 1$. The filters with $p < 1$ were designed based on the Butterworth element values, but the frequency responses have ripples (Fig. 8). Therefore, the filters are called

TABLE II
INDUCTANCE AND CAPACITANCE VALUES FOR THE BUTTER–CHEBY FILTER WITH $n = 4$, $f_0 = 1$ GHz, $Z_0 = 50\ \Omega$, AND $\Delta = 0.4$

p	1.1	1	0.9	0.8	0.7
L_1 (nH)	4.575	4.158	3.743	3.327	2.911
C_1 (pF)	5.537	6.090	6.767	7.613	8.701
L_2 (nH)	40.44	36.76	33.08	29.41	25.73
C_2 (pF)	0.626	0.689	0.766	0.861	0.984
L_3 (nH)	1.566	1.723	1.914	2.153	2.461
C_3 (pF)	16.17	14.70	13.23	11.76	10.29
L_4 (nH)	13.84	15.23	16.92	19.03	21.75
C_4 (pF)	1.830	1.664	1.497	1.331	1.165

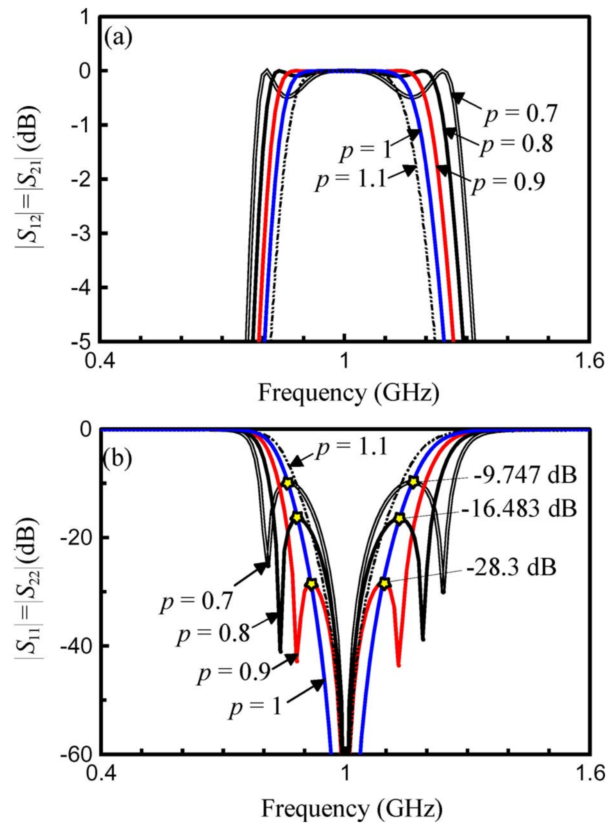

Fig. 8. Frequency responses of Butter–Cheby filters with $n = 4$. (a) $|S_{12}| = |S_{21}|$. (b) $|S_{11}| = |S_{22}|$.

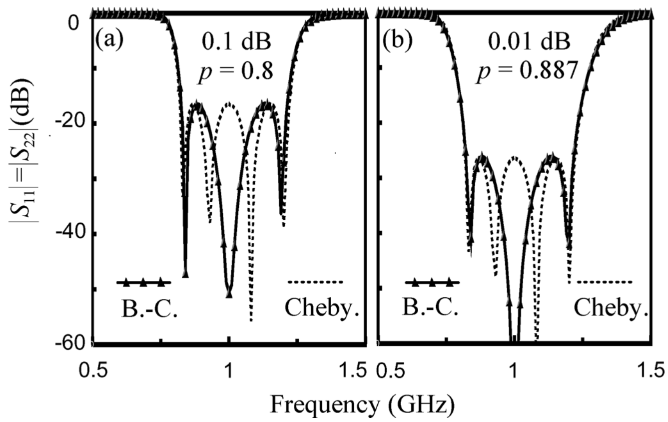

Fig. 9. Frequency responses of the Butter–Cheby filters with $n = 4$ are compared with the conventional Chebyshev filters. (a) 0.1-dB ripples. (b) 0.01-dB ripples.

TABLE III
INDUCTANCE AND CAPACITANCE VALUES FOR THE BUTTER–CHEBY FILTER WITH 0.01-dB RIPPLE

$p = 0.887$			
L_1 (nH)	4.9801	L_3 (nH)	2.6219
C_1 (pF)	5.0863	C_3 (pF)	9.6611
L_2 (nH)	24.153	L_4 (nH)	12.716
C_2 (pF)	1.0488	C_4 (pF)	1.9920

Butter–Cheby filters to distinguish from the conventional Butterworth or Chebyshev filters.

The Butter–Cheby filters are compared with two conventional Chebyshev filters in Fig. 9. The Chebyshev filters were chosen to have 0.01- and 0.1-dB insertion-loss ripples and the equi-ripple bandwidth 0.4. Note that the fractional bandwidth Δ is a 3-dB bandwidth and different from the ripple bandwidth defined by the Butter–Cheby or Chebyshev filter having ripples. The insertion losses of 0.01 and 0.1 dB are return losses of 26.383 and 16.4277 dB, respectively, under the assumption of lossless elements. From the frequency responses of Butter–Cheby filters in Fig. 8(b), to have 16.4277-dB return loss, p should be approximately 0.8. For 26.383-dB return loss, p should be between 0.8 and 0.9 [see Fig. 8(b)], and the exact value of p for the return loss is 0.887. With p close to unity, the ripple bandwidths become smaller. For a 40% Butter–Cheby filters with 0.01-dB ripple, $\Delta = 0.54$ is calculated, and for a 40% Butter–Cheby filters with 0.1-dB ripple, Δ is the same as that of the conventional Butterworth filter. That is, the fractional bandwidth of Δ is a parameter to design the Butter–Cheby filters, but the resulting ripple bandwidth of the Butter–Cheby filters is not always the same as the fractional bandwidth of the conventional Butterworth filter. Data of the Butter–Cheby filter with the 0.1-dB ripple are those with $p = 0.8$ and $\Delta = 0.4$ in Table II and those with 0.01-dB ripple in Table III.

The four filters are compared in Fig. 9 where the solid and dotted lines are the frequency responses of the Butter–Cheby and Chebyshev filters, respectively. The frequency responses with 0.1-dB ripple are in Fig. 9(a) and those with 0.01-dB ripple in Fig. 9(b). Two types of filter responses in Fig. 9 are identical in terms of bandwidths and skirt characteristics, but only pole locations are different. The results (Fig. 9) show that the Butter–Cheby filters can possess the advantages that both Chebyshev and Butterworth filters have; steeper roll-off, wider bandwidths, and equal termination impedances.

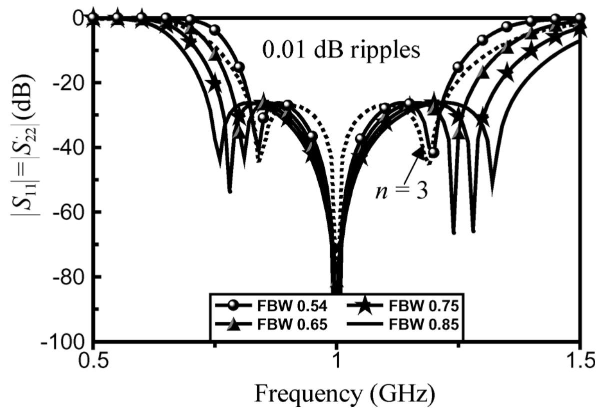

Fig. 10. Frequency responses of the Butter–Cheby filters with different bandwidths.

Varying p means changing the element values of the Butterworth low-pass prototype. If the element values of the Butter–Cheby filters are g_1', g_2', g_3', and g_4', they are connected with p such as

$$g_1' = g_4' = \frac{1}{p}g_1 = \frac{1}{p}g_4 \quad (16a)$$

$$g_2' = g_3' = pg_2 = pg_3. \quad (16b)$$

With p close to unity, the peak value of $|S_{11}|$ between two poles becomes smaller [see Fig. 8(b)]. This tendency is independent of the fractional bandwidth of Δ, but the frequencies where the two frequency responses with $p = 1$ and $p < 1$ intersect are dependent on the fractional bandwidth. The new element values of g_1', g_2', g_3', and g_4' in (16) can be used just like those of the conventional Chebyshev or Butterworth filters. For the Butter–Cheby filters with 0.01-dB ripple in Fig. 9(b), the new element values are $g_1' = g_4' = 0.862871$ and $g_2' = g_3' = 1.63896$.

Using them, four Butter–Cheby filters were additionally simulated by varying the factional bandwidths 0.54, 0.65, 0.75, and 0.85 and compared with the conventional Chebyshev filter with $n = 3$ in Fig. 10 where the frequency response with a dotted line is that of the conventional Chebyshev filter. The Butter–Cheby filter being compared to the Chebyshev filter with $n = 3$, number and location of the poles are about the same, but sharper slope characteristic is shown with the Butter–Cheby filter, as expected. The bandwidth of the Butter–Cheby filter with $\Delta = 0.85$ shows the widest, while that with $\Delta = 0.54$ shows the smallest. The frequency responses of the Butter–Cheby filters in Fig. 10 are the results scaled by the fractional bandwidths, or, the ripple bandwidths. The new elements of g_1' g_2', g_3', and g_4' may also be employed for termination impedance and frequency scaling as well.

D. Filter Design With $n = 6$

The Butter–Cheby filter with $n = 6$ may be considered as a filter that one filter with $n = 2$ is placed in the middle of another filter with $n = 4$. The values of p for $n = 4$ and q for $n = 2$ are

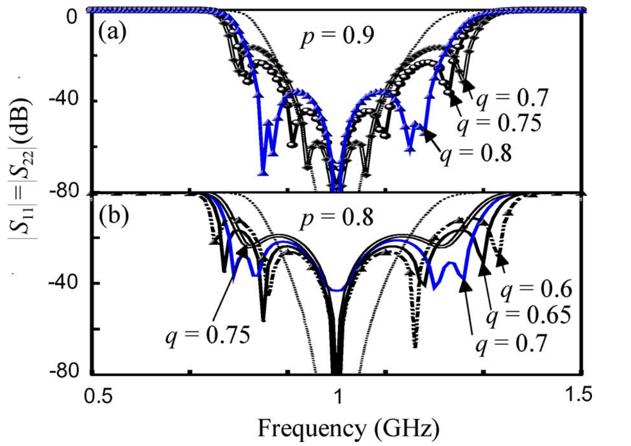

Fig. 11. Frequency responses of Butter–Cheby filters with $n = 6$. (a) $p = 0.9$. (b) $p = 0.8$.

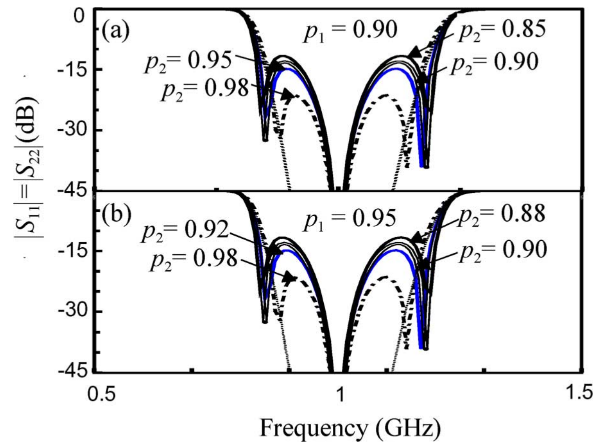

Fig. 12. Frequency responses of Butter–Cheby filters with $n = 8$. (a) $p_1 = 0.90$. (b) $p_1 = 0.95$.

therefore used. The following relations hold:

$$R_{(1,2)} = p\,R_{0(1,2)} \tag{17a}$$

$$g_3' = g_4' = qg_3 = qg_4 \tag{17b}$$

$$R_{(5,6)} = \frac{R_{0(5,6)}}{p}. \tag{17c}$$

Two types of simulation were carried out for the Butter–Cheby filters with $n = 6$ by fixing p and varying q. The simulation results are plotted in Fig. 11 where those with $p = 0.9$ and $p = 0.8$ are in Fig. 11(a) and (b), respectively. In both plots, the dotted lines without symbols are the conventional Butterworth filters. As expected, two poles are located at the design center frequency of 1 GHz and four others are located at other different frequencies. With $p = 0.9$ fixed in Fig. 11(a), when $q = 0.8$, two poles outside of the center frequency are located nearby and the peak value of $|S_{11}|$ between poles is -35.6 dB. With $q = 0.75$ and 0.7, those are -23.14 and -16.42 dB. With q smaller, the two poles outside of the center frequency are separated further. When $p = 0.8$ is fixed in Fig. 11(b), the two poles outside of 1 GHz are located nearby with $q = 0.7$ and separated further with q smaller. With $q = 0.75$, the two poles outside of the center frequency look like being overlapped. By the combination of p and q, the Butter–Cheby filters may be designed to satisfy the filter performance demanded.

E. Filter Designs With $n \geq 8$

The Butter–Cheby filter with $n = 8$ may be considered as a filter that one filter with $n = 4$ is placed in the middle of another filter with $n = 4$. Two different values of p_1 and p_2 are therefore needed. The following relations hold:

$$R_{(1,2)} = p_1\,R_{0(1,2)} \tag{18a}$$

$$R_{(3,4)} = p_2\,R_{0(3,4)} \tag{18b}$$

$$R_{(5,6)} = \frac{R_{0(5,6)}}{p_2} \tag{18c}$$

$$R_{(7,8)} = \frac{R_{0(7,8)}}{p_1}. \tag{18d}$$

Several Butter–Cheby filters with $n = 8$ were simulated by fixing p_1 and varying p_2, and the simulation results are plotted in Fig. 12 where those of the Butter–Cheby filters with $p_1 = 0.9$ and $p_1 = 0.95$ in Fig. 12(a) and (b), and thin dotted lines are the frequency responses of the conventional Butterworth filters with $\Delta = 0.4$. The frequency responses with $n = 8$ are very similar to those with $n = 4$ in Figs. 8–10. Four poles are overlapped at the design center frequency of 1 GHz, and two poles are degenerated at each pole location outside the design center frequency.

The Butter–Cheby filter with $n = 10$ may be seen as a filter where one filter with $n = 2$ is inserted into the center of another filter with $n = 8$. Three values of p_1, p_2, and q are therefore needed such as

$$R_{(1,2)} = p_1\,R_{0(1,2)} \tag{19a}$$

$$R_{(3,4)} = p_2\,R_{0(3,4)} \tag{19b}$$

$$g_5' = g_6' = qg_5 = qg_6 \tag{19c}$$

$$R_{(7,8)} = \frac{R_{0(7,8)}}{p_2} \tag{19d}$$

$$R_{(9,10)} = \frac{R_{0(7,8)}}{p_1}. \tag{19e}$$

The Butter–Cheby filters with $n = 10$ were simulated by varying p_1, p_2, and q and the simulation results are plotted in Fig. 13 where those of the Butter–Cheby filters with $p_2 = 0.9$ and $p_2 = 0.93$ in Fig. 13(a) and (b), and thin dotted lines are the frequency responses of the conventional Butterworth filters with $\Delta = 0.4$. The number of poles overlapped at the design center frequency is four and two poles are degenerated at each pole location outside the center frequency. Therefore, the pole locations of the Butter–Cheby filters with $n = 10$ are similar to those with $n = 6$.

The Butter–Cheby filter with $n = 12$ may be considered as a filter that one filter with $n = 4$ is inserted into the center of another filter with $n = 8$. That with $n = 14$ is regarded as a filter that one filter with $n = 2$ is located at the center of another filter with $n = 12$. Therefore, the concept may be expanded to the Butter–Cheby filters with an even number of resonators.

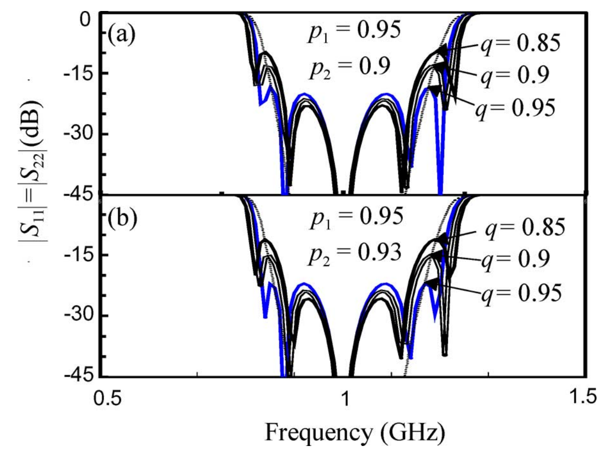

Fig. 13. Frequency responses of Butter–Cheby filters with $n = 10$. (a) $p_1 = 0.95$ and $p_2 = 0.90$. (b) $p_1 = 0.95$ and $p_2 = 0.93$.

TABLE IV
ELEMENT VALUES FOR THE BUTTER–CHEBY FILTERS WITH $n = 6$

$n = 6$				
$g_1 = g_6 = 0.517$, $g_2 = g_5 = 1.414$, $g_3 = g_4 = 1.931$				
p	q	$g_1' = g_6'$	$g_2' = g_5'$	$g_3' = g_4'$
0.9	0.7	0.575	1.273	1.352
0.9	0.75	0.575	1.273	1.449
0.9	0.8	0.575	1.273	1.545
0.8	0.6	0.647	1.131	1.159
0.8	0.65	0.647	1.131	1.256
0.8	0.7	0.647	1.131	1.352
0.8	0.75	0.647	1.131	1.449

F. Influence of Variables (p and q) on Pole Locations

For $n = 6$, the element values $(g_1', g_2', \ldots g_6')$ for the Butter–Cheby filters in Fig. 11 are given in Table IV where $g_1, g_2, \ldots g_6$ are those of the conventional Butterworth filter. The conventional values are between 0.517 and 1.931, while those for the Butter–Cheby filters are greater than 0.157 and less than 1.931. When $p = 0.9$ in Fig. 11(a), two poles with $q = 0.7$ outside the center frequency are separated further than those with $q = 0.75$ or $q = 0.8$. When $p = 0.9$ fixed in Table IV, only g_3' is changed. The value of g_3' (1.352) with $q = 0.7$ is less than those with $q = 0.75$ or $q = 0.8$ and closer to unity. That is, if g_3' is closer to unity, the poles are located in wider range of frequencies in Fig. 11(a). When $p = 0.8$ and $q = 0.6$ in Table IV, since the value of g_3' is 1.159 and three values of g_1', g_2' and g_3' become closer to unity, their poles in Fig. 11(b) spread wider than those with $p = 0.9$ and $q = 0.7$ in Fig. 11(a). For the design of the Butter–Cheby filters, it is, therefore, important to make all the element values close to unity by varying p and q. When $p = 0.8$ and $q = 0.6$ in Fig. 11(b), the four poles outside the center frequency are located wider than any other case, but it is natural that the return-loss response deteriorates to connect two nearby poles naturally. Since the wider pole-location does not mean the wider bandwidth, any optimization is therefore desired for the Butter–Cheby filter designs.

For $n = 8, R_{0(1,2)} = 1.68, R_{0(3,4)} = 1.08, R_{0(5,6)} = 0.92$ and $R_{0(7,8)} = 0.59$. In this case, since the difference between $R_{0(3,4)}$ and $R_{0(5,6)}$ is very small, the possibility to choose $R_{(3,4)} = R_{(5,6)}^{-1}$ between two values of 1.08 and 0.92 is restricted, keeping the relation in (14). The same reason occurs for the Butter–Cheby filters with $n = 10$. Due to the reason, two poles are degenerated at each pole location in Figs. 12 and 13.

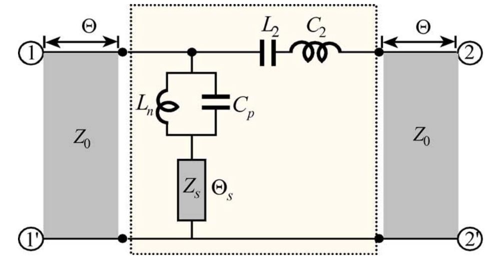

Fig. 14. Filter with $n = 2$ having a transmission zero.

IV. TRANSMISSION ZEROS

A. Transmission Zeros

The frequency responses of a filter with n even are not symmetric with respect to the center frequency and show gentler slope characteristic in the frequencies higher than the center frequency. Due to this, a transmission zero is needed, and a filter configuration with $n = 2$ for the transmission zero is depicted in Fig. 14 where a transmission-line section is inserted between a parallel resonator and ground. The parallel resonator (Fig. 14) with an inductance L_n and a capacitance C_p is connected in series with the transmission-line section having the characteristic impedance Z_s and the electrical length Θ_s. The impedance Z_t^s made by the parallel resonator and the transmission-line section is

$$Z_t^s = jZ_s \tan\Theta_s + \frac{j\omega L_n}{1-\omega^2 L_n C_p}. \tag{20}$$

To have a transmission zero f_{T0} outside of the resonance frequency, the impedance of Z_t^s needs to be zero, which leads to

$$Z_s \tan\Theta_s = \frac{\omega_{T0} L_n}{\omega_{T0}^2 L_n C_p - 1} \tag{21}$$

where $\omega_{T0} = 2\pi f_{T0}$.

To have the frequency response of the filter in Fig. 14 similar to that in Fig. 5 in the passband, the relation between these two types of filters in Figs. 5 and 14 holds

$$\frac{\omega L_1}{1-\omega^2 L_1 C_1} = Z_s \tan\Theta_s + \frac{\omega L_n}{1-\omega^2 L_n C_p}. \tag{22}$$

To satisfy the equation in (22), the following relation yields:

$$L_n C_p \cong L_1 C_1 = \omega_0^{-2}. \tag{23}$$

Equation (23) means that the design equations in (8)–(10) and (13)–(19) may be used for the transmission zeros. To satisfy the relation in (22), the transmission zero should be located at a frequency higher than the center (resonance) frequency.

B. Frequency Response With Transmission Zeros

To investigate the transmission-zero frequency f_{T0}, the filter with $n = 2$ was simulated by fixing the characteristic

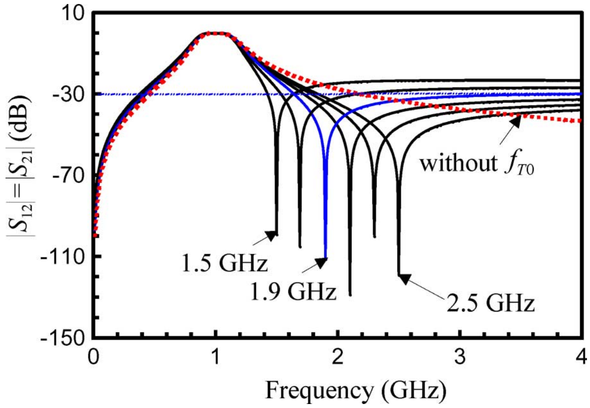

Fig. 15. Frequency responses with transmission zeros.

TABLE V
TRANSMISSION ZEROS OF THE BUTTER–CHEBY FILTER WITH $n = 2, Z_0 = 50\ \Omega, g_1' = g_2' = 1.3666$, AND $\Delta = 0.3$

$L_1 = L_n = 1.747$ nH, $C_1 = C_p = 14.5$ pF, $L_2 = 36.25$ nH and $C_2 = 0.69$ pF. $Z_s = 50\ \Omega$			
f_{T0} (GHz)	Θ_s (°)	f_{T0} (GHz)	Θ_s (°)
1.5	14.76°	1.7	11.17°
1.9	9.08°	2.1	7.70°
2.3	6.71°	2.5	5.97°

impedance Z_s to 50 Ω and varying the transmission-line length Θ_s (Fig. 15). In this case, the center frequency is 1 GHz, $Z_0 = 50\ \Omega, g_1' = g_2' = 1.3666$ and $\Delta = 0.3$. The resulting inductance and capacitance values are $L_1 = L_n = 1.747$ nH, $C_1 = C_p = 14.5$ pF, $L_2 = 36.25$ nH, and $C_2 = 0.69$ pF. The length of Θ_s is 14.76° at $f_{T0} = 1.5$ GHz, $\Theta_s = 5.79°$ at $f_{T0} = 2.5$ GHz, and is inversely proportional to f_{T0}. The calculation results are in Table V where Θ_s is the electrical length at its own transmission zero frequency. The filter responses are compared with and without the transmission zeros in Fig. 15 where the transmission zeros are really produced as designed. The frequency responses are almost the same with each other lower than 1 GHz, but different in the frequencies higher than the center frequency (Fig. 15). The frequency responses in Fig. 15 again verify that the design formulas without the transmission zeros in (8)–(10) and (13)–(19) may be used for the transmission zeros.

With $f_{T0} = 1.5$ GHz in Fig. 15, the transmission zero is located very close to the center frequency, but scattering parameter of $|S_{12}|$ again jumps up to less than -20 dB. When $f_{T0} = 2.5$ GHz, the transmission zero is a little bit far from the center frequency, but the final scattering parameter of $|S_{12}|$ after jumping up is less than -40 dB. Depending on applications such as multiplexers, the transmission-zero frequency can be adjustable.

V. REALIZATION

For the fabrication of the lumped-element Butter–Cheby filters, all the inductance and capacitance values required are not easy to get from the manufacturers. The series capacitances are of the biggest problem among the lumped elements because the filter performance is very sensitive to the series capacitance value and the capacitance needs to be realized as exactly as possible. The value of the series capacitance is also sometimes too small to be realized with commercial lumped elements, when the center (resonance) frequency of the filter increases. How to realize the series capacitances exactly with distributed elements only or distributed and lumped elements combined will be discussed. Further, other inductances and capacitances will also be investigated.

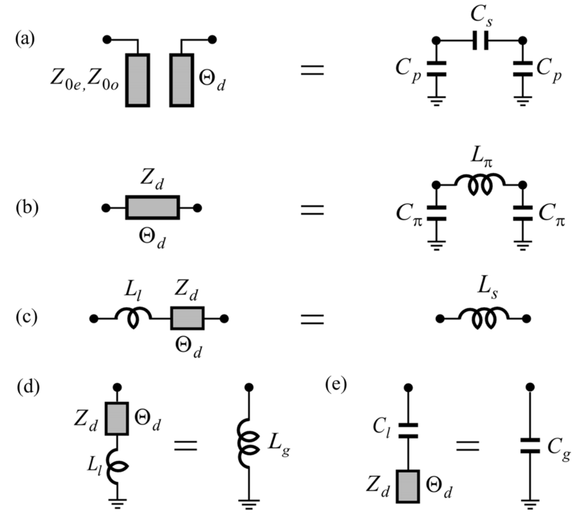

Fig. 16. Realization of capacitances and inductances. (a) Series capacitance. (b) and (c) Series inductance. (d) Shunt inductance. (e) Shunt capacitance.

A. Series Capacitance

One set of coupled transmission-line sections with two open circuits (distributed element) and its Π-type equivalent circuit (lumped element) are depicted in Fig. 16(a). The even- and odd-mode impedances of the coupled transmission-line sections are Z_{0e} and Z_{0o}, and the electrical length is Θ_d. The even- and odd-mode admittances Y_{OC} and Y_{SC} of the distributed element in Fig. 16(a) are

$$Y_{OC} = jY_{0e} \tan \Theta_d \tag{24a}$$
$$Y_{SC} = jY_{0o} \tan \Theta_d \tag{24b}$$

where $Y_{0e} = Z_{0e}^{-1}, Y_{0o} = Z_{0o}^{-1}$.

Those of the lumped equivalent circuit in Fig. 16(a) are

$$Y_{OC} = j\omega C_p \tag{25a}$$
$$Y_{SC} = j\omega C_p + j2\omega C_s. \tag{25b}$$

By equating the two equations in (24) and (25), the lumped element values of C_p and C_s are

$$\omega C_p = Y_{0e} \tan \Theta_d \tag{26a}$$
$$\omega C_s = \frac{Y_{0o} - Y_{0e}}{2} \tan \Theta_d. \tag{26b}$$

Applying $Y_{0o} = Y_{0e}(1 + C)/(1 - C)$ to (26), the relation between C_p and C_s is obtained as

$$C_s = C_p \left(\frac{C}{1 - C} \right) \tag{27}$$

where C is a coupling coefficient.

The electrical length Θ_d and the coupling coefficient associated with the lumped elements [see Fig. 16(a)] are therefore obtained as

$$\Theta_d = \tan^{-1}(\omega C_p \cdot Z_{0e}) \tag{28a}$$
$$C = \frac{C_s}{C_s + C_p}. \tag{28b}$$

To realize the series capacitance with the distributed element [see Fig. 16(a)], the shunt capacitance of C_p should be so small to be regarded as an open circuit. If the value of $(\omega C_p)^{-1}$is more than 400 Ω, the distributed element may be equivalent to the series capacitor of C_s only [see Fig. 16(a)]. To have higher value of $(\omega C_p)^{-1}$, the even-mode impedance of Z_{oe} should be chosen as high as possible and the length of Θ_d as small as possible. The distributed element may then be equivalent to the series capacitance of C_s only. The capacitance produced by the distributed element is generally small and becomes smaller with the operating frequency higher. The series capacitance of the filters in Figs. 5 and 7 may be realized with distributed elements and lumped elements combined together.

B. Other Values

To have exact values of series inductance L_s, shunt inductance L_g, and shunt capacitance C_g in Fig. 16, lumped elements and transmission-line sections combined together may be used. A transmission-line section with the characteristic impedance of Z_d and electrical length of Θ_d may be equivalent to a circuit consisting of a series inductance L_π and two identical shunt capacitances C_π [13] in Fig. 16(b). Their values are expressed as

$$\omega L_\pi = Z_d \sin\Theta_d \tag{29a}$$
$$\omega C_\pi = \frac{1}{Z_d}\tan\frac{\Theta_d}{2}. \tag{29b}$$

For the equivalent circuit [see Fig. 16(b)], absolute reactance value of $(\omega C_\pi)^{-1}$ is 685 Ω with $\Theta_d = 10^\circ$ and $Z_d = 60\ \Omega$, while $(\omega C_\pi)^{-1}$ is 3437 Ω with $\Theta_d = 2^\circ$ and $Z_d = 60\ \Omega$. When $\Theta_d = 10^\circ$ and $Z_d = 140\ \Omega, (\omega C_\pi)^{-1}$ is 1660 Ω, while $(\omega C_\pi)^{-1}$ is 8020 Ω with $\Theta_d = 2^\circ$ and $Z_d = 140\ \Omega$. If Z_d is greater than 60 Ω and Θ_d is less than 10°, the transmission-line section [see Fig. 16(b)] may therefore be considered as a series inductance of L_π only. Due to the fact, the series inductance L_s in Fig. 16(c) may be obtained as

$$\omega L_s = \omega L_l + Z_d \sin\Theta_d \tag{30}$$

where L_l is a lumped element given by the manufacturers.

The exact values of the shunt inductance L_g and shunt capacitance C_g connected to the ground in Fig. 16(d) and (e) may also be obtained by lumped elements of L_l and C_l and transmission-line sections combined together, as shown in Fig. 16(d) and (e). The inductance of L_g is greater than L_l, but the capacitance of C_g is less than C_l.

VI. Measurements

To verify the design method, one microstrip Butter–Cheby filter with 0.01-dB ripple was fabricated on a substrate (RT/Duroid 5870, $\varepsilon_r = 2.33, H = 0.787$ mm) with lumped and distributed elements. The data in Tables III were therefore used for the fabrication. If the designed values of the capacitances or inductances meet those supplied by the manufactures, lumped elements only were employed for the fabrication. Otherwise, distributed and lumped elements were combined. The lumped elements supplied by American Technical Ceramics (ATC) were

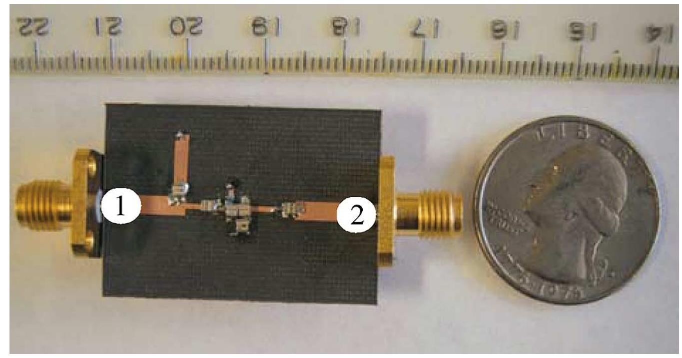

Fig. 17. Fabricated Butter–Cheby filter.

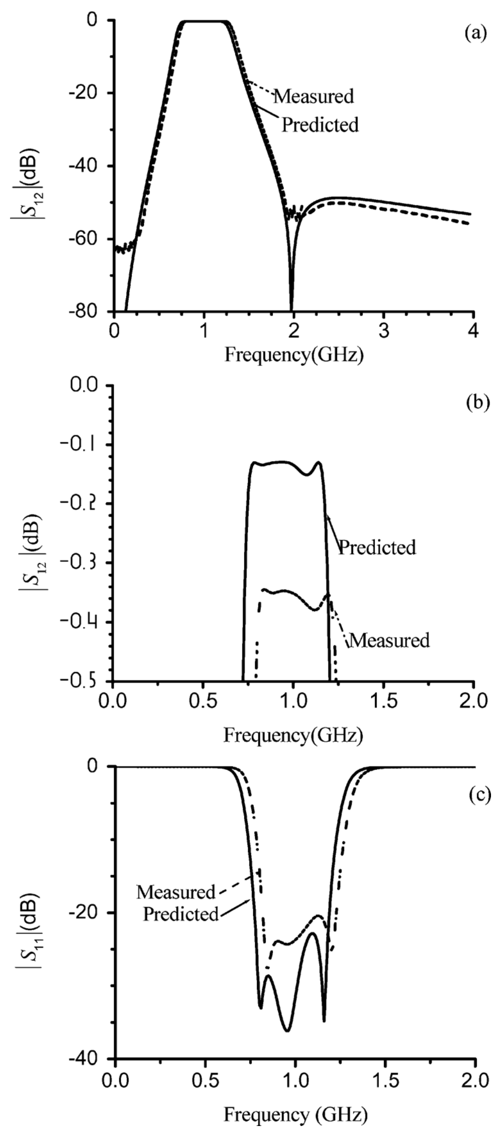

Fig. 18. Results measured and predicted are compared. (a) and (b) $|S_{21}| = |S_{12}|$. (c) $|S_{11}| = |S_{22}|$.

utilized based on the data sheets giving scattering parameters from 0.05 to 20 GHz. A transmission-line section for the transmission zero was inserted between a parallel resonator with L_1 and C_1 (Fig. 7) and ground to have $f_{T0} = 2$ GHz. The capacitances and inductances of L_1, C_1, and C_4 (Table III) were fabricated with lumped elements only because of $L_1 = 5$ nH, $C_1 = 5$ pF, and $C_4 = 2$ pF. The other values were realized by the combination of distributed and lumped elements. The inductance of $L_2 = 24.15$ nH is made of a lumped inductor of $L_l = 23$ nH and a transmission-line section with $Z_d = 130\ \Omega$ and $\Theta_d = 4°$ [see Fig. 16(c)]. That of $L_3 = 2.6219$ nH consists of a lumped inductor of 2 nH and a transmission-line section with $Z_d = 100\ \Omega$ and $\Theta_d = 2.2°$. That of $L_4 = 12.716$ nH comprises a lumped inductor of 12 nH and a transmission-line section with $Z_d = 100\ \Omega$ and $\Theta_d = 2.6°$. That of $C_3 = 9.66233$ pF is fabricated with a lumped capacitor of 9 pF connected in parallel with another capacitance of 0.66 pF. The capacitance of 0.66 pF is realized with the form of C_g [see Fig. 16(e)] where $C_l = 5$ pF, $Z_d = 40\ \Omega$, and $\Theta_d = 9.7°$. The fabricated Butter–Cheby filter is displayed in Fig. 17 and the frequency responses measured and predicted are compared in Fig. 18 where frequency responses of scattering parameter of $|S_{21}| = |S_{12}|$ are in Fig. 18(a) and (b) and those of $|S_{11}| = |S_{22}|$ are in Fig. 18(c). As designed, the transmission zero is located around 2 GHz, and the measured return and insertion losses are better than 20 and 0.4 dB, respectively. In general, the measured results are in good agreement with the predicted ones, given fabrication errors.

VII. Conclusion

In this paper, a new design method for the BPFs with an even number of resonators has been suggested for compacter size and wider bandwidth. The filters designed in this paper can be terminated in equal impedances and may have ripple responses at the same time. The resulting filter characteristics are therefore quite different from those of the conventional Chebyshev and Butterworth filters, and the filters suggested in this paper are called Butter–Cheby filters to characterize their own properties. The element values for the Butter–Cheby low-pass prototype can be generated arbitrarily depending on the filter performance and scaled by bandwidth, frequency, and termination impedances. The element values of the Butter–Cheby filters may be obtained easily, by which bandpass, bandstop, and low-pass Butter–Chebyshev filters are also possible for the compacter size and wider bandwidths.

References

[1] H.-R. Ahn and T. Itoh, "Design method for a lumped-element bandpass filter with two resonators and its application to multiplexers," *IET Microw., Antennas, Propag.*, vol. 5, no. 7, pp. 804–810, 2011.

[2] H.-R. Ahn and T. Itoh, "Multiplexers using unit-cell filters of CRLH TLs," in *Asia–Pacific Microw. Conf. Dig.*, 2010, pp. 674–677.

[3] S. Hong and K. Chang, "A 10–35 GHz six-channel microstrip multiplexer for wideband communication systems," *IEEE Trans. Microw. Theory Tech.*, vol. 54, no. 4, pp. 1370–1378, Apr. 2006.

[4] J.-A. Gong and W.-K. Chen, "Computer-aided design of a singly-matched (S-M) multiplexer with a common junction," *IEEE Trans. Microw. Theory Tech.*, vol. 41, no. 5, pp. 886–890, May 1993.

[5] P. M. Latourrette and J. L. Roberds, "Extended-junction combline multiplexers," in *IEEE MTT-S Int. Microw. Symp. Dig.*, 1978, pp. 214–216.

[6] H.-R. Ahn and S. Nam, "Wideband coupled-line microstrip filters with high impedance short-circuited stubs," *IEEE Microw. Wireless Compon. Lett.*, vol. 21, no. 11, pp. 586–588, Nov. 2011.

[7] J. D. Rhodes and R. Levy, "A generalized multiplexer theory," *IEEE Trans. Microw. Theory Tech.*, vol. MTT-27, no. 2, pp. 99–111, Feb. 1979.

[8] P. M. Shankar, "Quantitative measures of boundary and contrast enhancement in speckle reduction in ultrasonic B-mode images using spatial Bessel filters," *IEEE Trans. Ultrason., Ferroelectr., Freq. Control*, vol. 56, no. 10, pp. 2086–2096, Oct. 2009.

[9] U.-K. Moon and B.-S. Song, "Design of a low-distortion 22-kHz fifth-order Bessel filter," *IEEE J. Solid-State Circuits*, vol. 28, no. 12, pp. 1254–1264, Dec. 1993.

[10] H.-R. Ahn and T. Itoh, "Impedance-transforming symmetric and asymmetric DC blocks," *IEEE Trans. Microw. Theory Tech*, vol. 58, no. 9, pp. 2463–2474, Sep. 2010.

[11] J.-S. Hong and M. J. Lancaster, *Microstrip Filters for RF/Microwave Applications*. New York: Wiley, ch. 3.

[12] G. L. Matthaei, L. Young, and E. M. T. Jones, *Microwave Filters, Impedance-Matching Networks and Coupling Structures*. Norwood, MA: Artech House, 1980.

[13] H.-R. Ahn, *Asymmetric Passive Components in Microwave Integrated Circuits*. New York: Wiley, 2006, p. 78.

[14] D. M. Pozar, *Microwave Engineering*. New York: Wiley, pp. 481–483.

Hee-Ran Ahn (S'90–M'95–SM'99) received the B.S., M.S., and Ph.D. degrees in electronic engineering from Sogang University, Seoul, Korea, in 1988, 1990, and 1994, respectively.

Since April 2011, she has been with the School of Electrical Engineering and Computer Science, Seoul National University, Seoul, Korea. From August 2009 to December 2010, she was with the Department of Electrical Engineering, University of California at Los Angeles (UCLA). From July 2005 to August 2009, she was with the Department of Electronics and Electrical Engineering, Pohang University of Science and Technology, Pohang, Korea. From 2003 to 2005, she was with the Department of Electrical Engineering and Computer Science, Korea Advanced Institute of Science and Technology (KAIST), Daejeon, Korea. From 1996 to 2002, she was with the Department of Electrical Engineering, Duisburg–Essen University, Duisburg, Germany, where she was involved with the habilitation dealing with asymmetric passive components in microwave circuits. She authored *Asymmetric Passive Component in Microwave Integrated Circuits* (Wiley, 2006). Her interests include high-frequency and microwave circuit design and biomedical application using microwave theory and techniques.

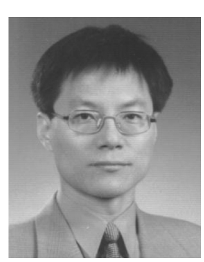

Sangwook Nam (S'87–M'88–SM'11) received the B.S. degree from Seoul National University, Seoul, Korea, in 1981, the M.S. degree from the Korea Advanced Institute of Science and Technology (KAIST), Seoul, Korea, in 1983, and the Ph.D. degree from The University of Texas at Austin, in 1989, all in electrical engineering.

From 1983 to 1986, he was a Researcher with the Gold Star Central Research Laboratory, Seoul, Korea. Since 1990, he has been a Professor with the School of Electrical Engineering and Computer Science, Seoul National University. His research interests include analysis/design of electromagnetic (EM) structures, antennas and microwave active/passive circuits.